

# Micromechanics simulations of the viscoelastic properties of PBX-9501 by material point method

*Liping Xue, Oleg Borodin, Grant D. Smith and John Nairn  
University of Utah, Salt Lake City, UT 84112*

## Abstract

Viscoelastic properties of the highly filled plastic-bonded explosive PBX-9501 were studied by two-dimensional dynamic Material Point Method (MPM) simulations. The upper and lower bounds for the composite properties were estimated from iso-displacement and iso-stress boundary conditions. A homogenized or “dirty” binder approach was utilized to handle the multiple length scales involved in MPM simulations of highly-filled composites with a broad distribution of filler particle sizes. Multiple time scale challenges were addressed by conducting a series of simulations in which the speed of sound of the composite was systematically varied by adjusting material point masses. This approach was used to predict the homogenized time-dependent shear modulus of PBX-9501 from nanoseconds to milliseconds yielding good agreement with experimental data.

## Introduction

PBX-9501 is a heterogeneous explosive material that consists of 95 wt% (93.7 vol%) elastic HMX (octahydro-1,3,5,7-tetranitro-1,3,5,7-tetrazocine) grains and 5 wt% (6.3 vol%) polymer binder, which is a 1:1 mixture of the rubber estane 5703 and a plasticizer BDNPA/F (bis(2,2-dinitropropyl)acetal/bis(2,2-dinitropropyl) formal). The mechanical behavior of the binder is strain rate, temperature and pressure dependent. As a result, the response of PBX 9501 also depends on strain rate, temperature and pressure. An understanding of the viscoelastic properties of PBX-9501 as a function of strain rate and temperature is critical to the understanding and prediction of the non-shock ignition of this type of material, which is important in safety assessments of handling and assembly of weapons systems. Due to the explosive nature of PBX-9501 experimental testing is difficult and expensive. Unfortunately, existing theoretical approaches that have been successfully applied to more conventional composites have not been successful for PBX-9501 [1,2]. The huge contrast (up to four magnitudes or higher) in mechanical properties between the binder and HMX, and the high volume fraction and extremely broad size distribution (ranging from sub-micron to millimeters in diameter) [3] of the HMX particles contribute to the failure of theoretical analysis.

Because of the intrinsic difficulties associated with experimental investigations and application of existing theories, numerical simulations that explicitly consider the composite microstructure are expected to play a more important role in predicting mechanical response of PBX-9501 than they play in the studies of conventional composites [2,4-6]. Such homogenization simulations of PBX-9501, however, are complicated by a number of factors including: a) the need to realistically represent PBX-9501 microstructure with a broad distribution of filler sizes necessitating the use of a huge number of small computational elements; b) complicated geometries of HMX particles; c) the need to predict PBX-9501 viscoelastic response over times ranging from picoseconds to seconds.

Our main goal is to design an efficient simulation methodology for obtaining the viscoelastic response of PBX-9501 and similar highly filled polymer composites over a wide range of response times utilizing the properties of the constituents and microstructure of the composite as input. In this paper we present a combination of methods for efficient handling of a broad filler particle size distribution in homogenization simulations and a method for handling multiple time scales that will

allow us to obtain PBX-9501 shear modulus from nanoseconds to milliseconds. The idea behind the homogenization approach is that mechanical properties of the binder can be replaced with an effective (homogenized) binder containing the smallest particle and used in larger-scale simulations where only the larger particles are explicitly represented, requiring much coarser resolution and, therefore, significantly less computational time. The procedure is repeated until the homogenized binder represents the response of the binder and all but the largest particles, which are still represented explicitly. Results of this final simulation yield the homogenized properties of the composite. Finally, variation of the speed of sound of the material through adjustment of the masses of the material points allows us to probe the viscoelastic response of the PBX-9501 over a wide range of times scales much more efficiently than would be possible utilizing fixed masses and a single, long simulation.

We have chosen dynamic material point method (MPM) [7-10] for property homogenization because it offers some advantages over other numerical techniques for simulations of mechanical properties of composites with complicated geometries found in PBX-9501. In MPM it is very easy to discretize complex geometries of composites compared to mesh generation needed for FEM calculations. MPM also has been successful in solving problems involving large deformation and contact, having an advantage over traditional FEM [11], because the fixed regular grid employed by MPM eliminates the need for doing costly searches for contact surfaces and/or re-meshing by FEM.

## **MPM Simulation Methodology**

MPM simulations were performed utilizing the two-dimensional NairnMPM code [12]. In all simulations the composites are comprised of an ensemble of relatively stiff circles representing filler particles within a viscoelastic matrix. A linear viscoelastic constitutive material model has been implemented in the NairnMPM code for the plain-strain 2-D approximation, which is used in all MPM simulations. The time step was set to  $0.1 d/c$ , where  $d$  is the dimension of the elements in the background grid,  $c$  is the wave speed for the material with the largest compressibility. Four material points were used per each background element. Both regular and random composites were studied. In regular composites the particles were placed on a regular array within the matrix. For random composites the Lubachevsky-Stillinger algorithm [13] was used to pack filler particles.

### ***Determination of the Viscoelastic Response of the Composites***

We mimic two common experimental techniques to obtain the time-dependent viscoelastic behavior of the composites from MPM simulations: the stress relaxation experiment and the creep experiment. For stress relaxation simulation, as shown in Fig. 1, a shear strain is applied over a short period of time and maintained throughout the simulation. The strain is uniform over the entire boundary (iso-strain boundary conditions). The shear stress is then monitored as a function of time. The time-dependent shear modulus  $G(t)$  then is obtained from the stress/strain relation. Initial fluctuations seen in Fig. 1(c) of the time dependent shear modulus are due to incomplete propagation of stress waves through the material. We typically wait for stress waves to travel back and forth at least 3 times through the simulation cell before collecting material response data. The magnitude of the applied strain is chosen on the order of  $10^{-6}$ - $10^{-8}$ , i.e., small enough to provide minimum perturbation to the volume and shape of the composite but not so small as to influence numerical accuracy of the stress response of the material.

For creep experiment simulations a shear stress is applied over a short period of time at the beginning of the simulation and then maintained uniform over the entire boundary (iso-stress boundary conditions). The shear strain is then monitored as a function of time. The behavior of the sample is analogous to that shown in Fig. 1. The time-dependent shear compliance  $J(t)$  then is obtained from the

stress/strain relation. Using the Boltzmann superposition principle and Laplace transformation [14], the shear modulus  $G(t)$  can be obtained from the compliance  $J(t)$  and vice-versa.

Theoretically, stress relaxation simulations with iso-strain boundary conditions corresponds to the minimum potential energy principle [15,16]. Correspondingly, the shear modulus  $G(t)$  predicted by the stress relaxation simulation gives an upper bound of composite modulus. Creep experiment simulations with iso-stress boundary conditions corresponds to the minimum complementary energy principle [15,16]. The shear compliance  $J(t)$  and shear modulus  $G(t)$  predicted from these experiments give a lower bound of composite modulus.

In the following discussions, only stress relaxation simulation results are used in investigation of the sensitivity of composite properties to material point resolution, the size of the RVE and validation of the homogenized binder approximation. The creep simulations showed similar trends and are not presented. Results of stress relaxation simulations yielding an upper bound and creep simulations yielding a lower bound of the PBX-9501 modulus are presented.

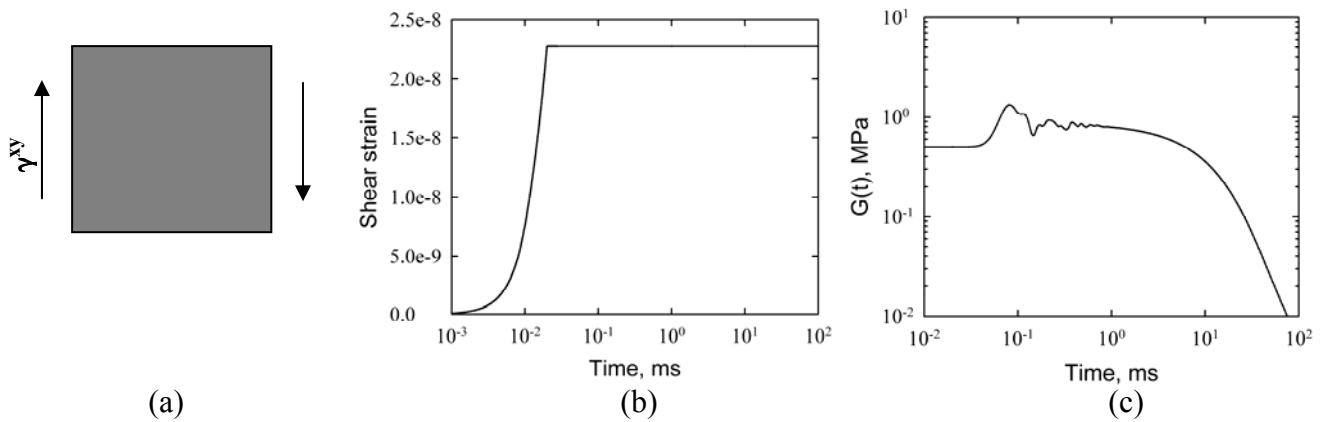


**Figure 1.** Illustration of the stress relaxation simulations. (a) Schematic of composite shear strain loading. (b) Shear strain loading curve. (c) Shear modulus from shear stress relaxation.

### ***Sensitivity of Composite Modulus to MPM Spatial Resolution***

The accuracy of the MPM predictions of composite properties depends on the material point (MP) density (resolution) governing resolution of the filler/binder interfaces. MPM simulations were performed in order to investigate the sensitivity of composite properties on the accuracy of the description of stress/strain transfer through the filler/binder interface for fillers evenly spaced and well-separated from each other shown in Fig. 2 using model composites with constituent properties given in Table 1. For the model composites the ratio of the shear modulus of the filler particle to the shear modulus of the matrix mimics that found in PBX-9501 but for computational expediency the viscoelastic modulus of the matrix has a much simpler constitutive equation. Analysis of Fig. 2 indicates that at short times, where the difference between the shear modulus of the fillers and matrix is relatively small, that  $G(t)$  for the composite shows little dependence on resolution. However, for longer times, where the modulus of the matrix has decayed appreciably,  $G(t)$  of the composite becomes resolution dependent and monotonically decreases as spatial resolution increases, a behavior similar to the findings of previous FEM simulations [4]. The relative deviation  $(G(t)-G^{\text{eff}}(t))/G^{\text{eff}}(t)$  of the composite shear modulus calculated at a given resolution is also plotted in Fig. 2, where  $G^{\text{eff}}(t)$  is the effective  $G(t)$  and from the one calculated using the highest resolution of 66 MP/mm. The ratio  $(G(t)-G^{\text{eff}}(t))/G^{\text{eff}}(t)$  increases with increasing filler/matrix contrast and decreases with increasing resolution.

We observe that increasing of resolution by a factor of two decreases  $(G(t)-G^{\text{eff}}(t))/G^{\text{eff}}(t)$  by about a factor of  $\approx 2.3$  for all filler/matrix contrasts.

**Table 1.** Material parameters of the model composites

Binder		
	Bulk Modulus $K$	1.0 MPa
	Shear Modulus $G$	$0.5e^{-t/0.01}$ MPa, time unit: second
	Density $\rho$	$1.0 \text{ g/cm}^3$
Particle		
	Bulk Modulus $K$	50 MPa
	Shear Modulus $G$	18.8 MPa
	Density $\rho$	$1.5 \text{ g/cm}^3$

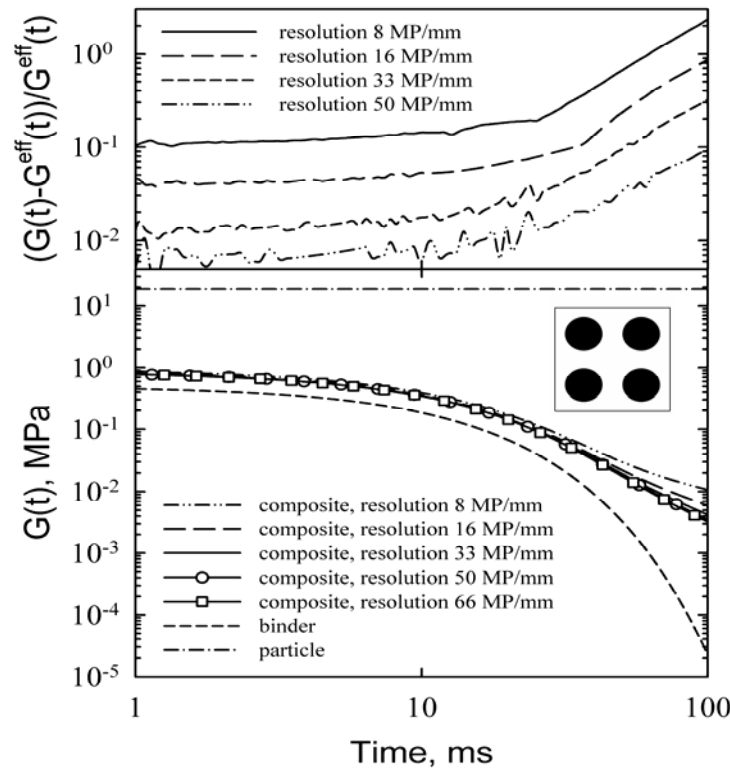


**Figure 2.** Composite shear modulus  $G(t)$  for various resolutions and deviation  $(G(t)-G^{\text{eff}}(t))/G^{\text{eff}}(t)$  from  $G^{\text{eff}}(t)$  calculated using 66 MP/mm resolution. A particle diameter is 2 mm, length of the box is 6.0 mm.

We suppose that stiffening of the overall composite shear modulus  $\Delta G(t)/G(t)$  due to insufficiently resolved interfacial stress/strain transfer in our computational experiments is proportional to the amount of the interfacial polymer given by  $L*W$ , where  $L$  is the length of the interface per area and given by  $S/A$ , where  $S$  is the total length of the interface and  $A$  is the total area of the simulation box, and  $W$  is the width of the interfacial polymer that has a significantly stiffer modulus due to insufficient resolution. We note that  $W \sim 1/R$ , where  $R$  is the density of MP (resolution). Thus,  $\Delta G(t)/G(t) \sim S/(AR)$ . Fig. 2 demonstrated that  $\Delta G(t)/G(t) \sim S/(AR)$  holds for constant  $S$  and  $A$ . Fig. 3 demonstrates that  $\Delta G(t)/G(t) \sim S/(AR)$  holds for various  $S$  and  $R$  by changing interfacial length while

keeping the filler area fraction constant. Indeed, doubling MP resolution and increasing interfacial length leaves  $\Delta G(t)/G(t)$  largely unchanged.

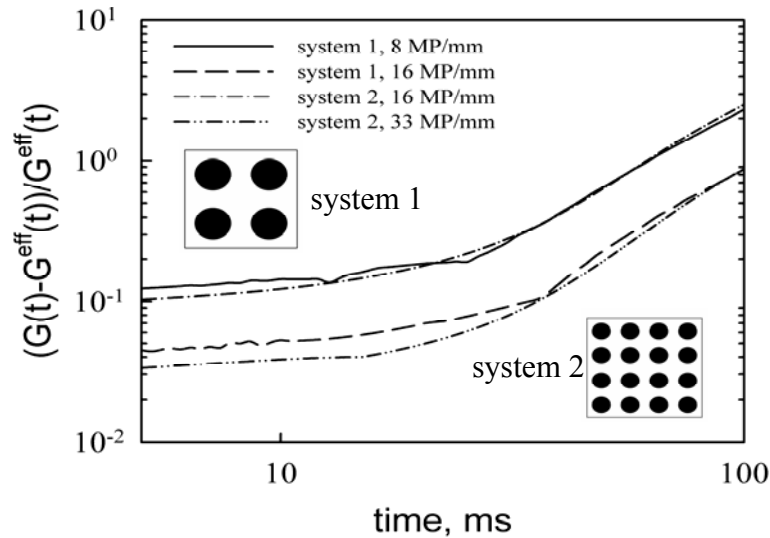


**Figure 3.** Deviation  $\Delta G(t)$  from  $G^{\text{eff}}(t)$  for two composites with the same filler area fraction but interfacial length different by a factor of two by reducing the diameter of the filler by a factor of two and increasing the number of fillers by a factor of four while keep the box size unchanged. The  $G^{\text{eff}}(t)$  are taken from the resolutions that also different by a factor of two for the two different composites to make the comparison reasonable.

Special care must be taken for choosing resolution for composites with matrix closely confined by fillers. For example, if discretization of confined matrix between fillers results in two MP from different fillers next to each other, two fillers will be effectively touching each other as MPM realizes no slip contact. This contact will result in a higher composite modulus as previous FEM simulations [5] showed that the composite with aggregated (touching) particles has a higher modulus than the random composite because of improved stress transfer from particle to particle at points of particle contact. We summarize by stating that two criteria should be addressed in order to choose adequate resolution for homogenization simulations: a) sufficient resolution of the filler-particle interface for fillers well separated from each other by the binder, the relation  $\Delta G(t)/G(t) \sim S/(AR)$  could be used to obtain estimates of required resolution; and b) sufficient resolution of interfacial matrix confined between solid filler interfaces, usually requiring four and more MP to represent confined matrix.

### ***Effect of Variation in Random Packing on Composite Properties***

Because the MPM simulations involve a finite number of particles, it is possible that composite properties will vary from one microstructure to another created by random packing configurations utilizing the same set of particles. In order to investigate the influence of random packing configuration on composite properties, a representative model composite consisting of 25 filler particles of diameter 0.1 mm packed in a 0.6 x 0.6 mm square cell, corresponding to a filler volume (area) fraction of 55%, was studied, utilizing properties given in Table 1. The resolution was set to 330 MP/mm and a spacing of at least 10 material points between particles was maintained in order to guarantee the insensitivity of simulation results to MP resolution. The microstructures of the three different composites and the corresponding shear moduli  $G(t)$  are shown in Fig. 4. At early times, corresponding to small filler/binder contrast, the three composite structures yield essentially the same

shear modulus. At longer times differences become apparent. However, even when the contrast between constituent modulus is large (e.g., more than 5 orders of magnitude at 100 ms), less than 10% difference in the composite  $G(t)$  is observed. This is consistent with observations of previous FEM simulations [4] that a rather small size of RVE is needed to represent random composites.

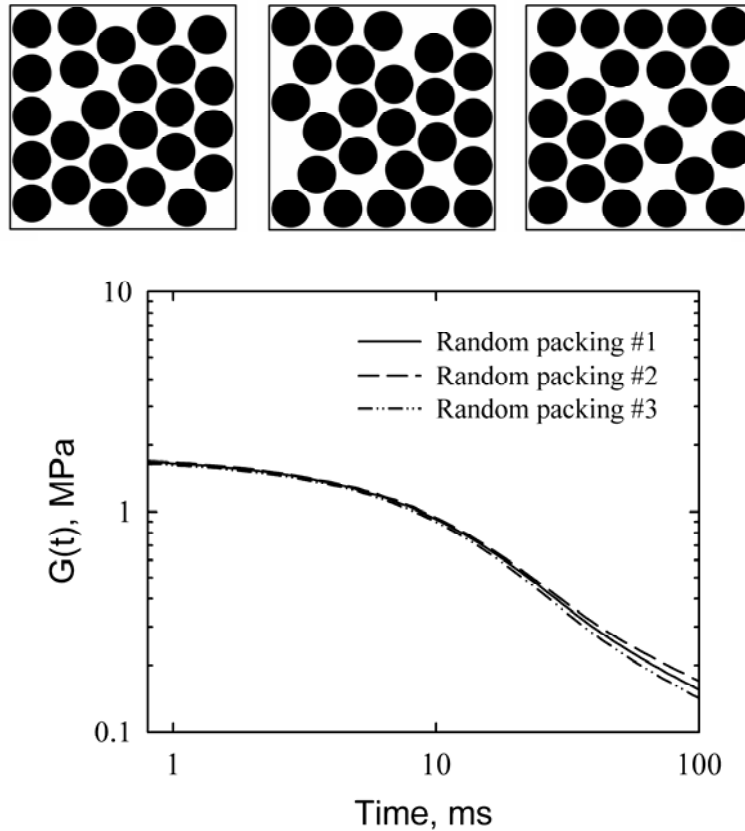


**Figure 4.** Effect of different packings to the viscoelastic properties.

### ***Homogenized “Dirty” Binder Approximation***

Because of a large volume fraction and very broad size distribution of HMX particles, simulations of PBX-9501 require at least  $10^{+8}$  material points in order to properly resolve the smallest particles of 2.0  $\mu\text{m}$  diameter for an RVE of 2.75mm. We have therefore utilized a homogenized, or “dirty”, binder approximation that allows us to successively subsume increasingly larger particles into an effective matrix whose properties include the influence of the subsumed particles. In other words, we assume that the binder with the smaller particles (homogenized binder) can be represented as a continuum with homogenized properties and can be used in simulations where only larger particles are explicitly represented.

The accuracy of the homogenized binder approximation was investigated for regular and random composites with particles completely coated by the binder (no particle contact within 6 MP) and is demonstrated in Fig. 5 for the model composite (Table 1). The composites have a total particle volume (area) fraction of 57%. We performed separate simulations of a composite consisting of only small particles and all of the binder (homogenized binder). The properties of the homogenized binder were subsequently used in composite simulations with the larger particle. For comparison we also performed simulations of a composite with both small and large particles explicitly included. Fig. 5 indicates that composite properties with the homogenized binder are quite similar to those obtained from simulation where all particles are resolved simultaneously, with the simulations utilizing the

homogenized binder predicting slightly lower modulus at long time. Simulations for the composite with much higher particle volume (area) fraction of 73.7% exhibit similar results. These results show that, at least for the cases studied, the implicit homogenized binder approximation does not introduce significant errors and can be applied even when the volume fraction of particles to be subsumed into the binder is very high.

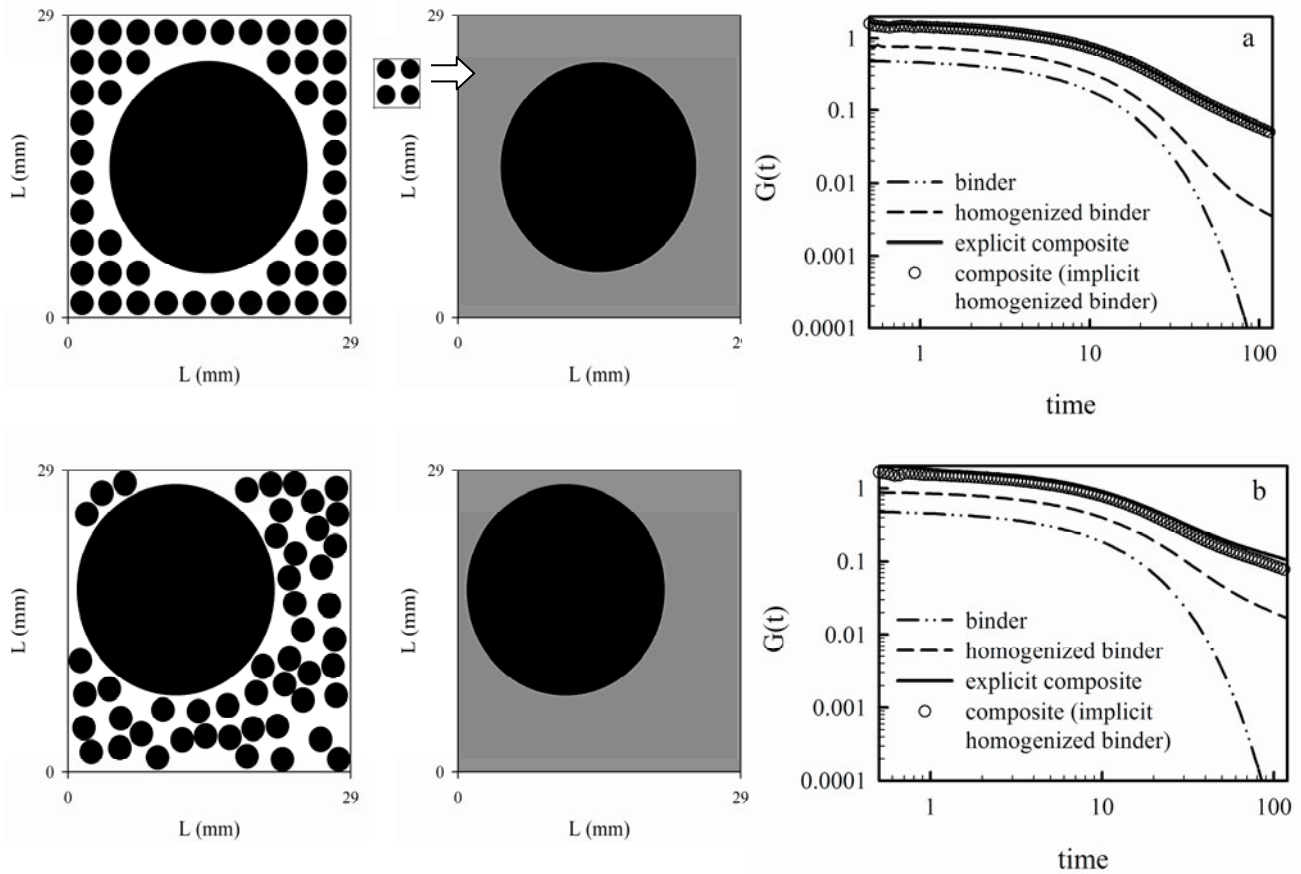


**Figure 5.** Validation of the homogenized binder approximation for regular and random composites. The simulation box size is 29\*29 mm and contains totally 57 vol% particles. The small particle has a diameter of 2 mm and the large particle has a diameter of 20 mm. The volume fraction of homogenized binder (small particles in the pure polymer) is 30 vol%.

### ***Multiple Time Scale Simulations***

We are interested in the time dependent shear modulus  $G(t)$  of PBX-9501 from times ranging from  $10^{-5}$  to  $10^{+1}$  milliseconds or even longer. It is not feasible to cover this time domain in a single simulation for a typical RVE. In order to overcome this multiple time scale challenge we varied the material speed of sound within the composite by changing both filler and binder density through variation of the MP masses. As the speed of the sound in the material is given by  $\sqrt{E/\rho}$ , the time step in the explicit MPM solution is proportional to  $\sqrt{\rho}$ , where  $E$  is the young's modulus and  $\rho$  is the density of the material. By changing the density of the material we can change the time step without changing the viscoelastic response of the composite on time scales long compared to the time it takes for a stress wave to propagate through the simulation cell. Fig. 6 demonstrates that the homogenized composite modulus is almost independent of the wave speed of probing perturbations.

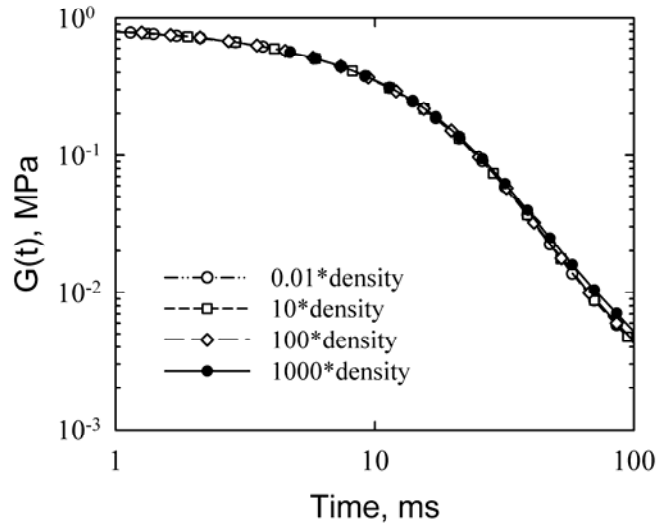


Figure 6. Effect of density (composite speed of sound) on the effective viscoelastic properties from MPM simulations. Composite configuration from Fig. 3 was used.

### Prediction of $G(t)$ for PBX-9501

The constituent properties for PBX-9501 are given in Table 2 and correspond to a temperature of 19 °C. In our PBX-9501 simulations we divide particles into three classes of sizes, as shown in Fig. 7. First, properties of the binder plus the smallest particles (particle size less than 14  $\mu\text{m}$ ), called homogenized binder 1 (HB-1) in this paper (see Fig. 7c), are obtained.  $G(t)$  for HB-1 is then used in simulations with the intermediate size particles (particle size from 14  $\mu\text{m}$  to 100  $\mu\text{m}$ ) to obtain homogenized properties of the binder with small and intermediate size particles (HB-2, Fig. 7d). Finally, simulations involving the largest particles (particle size larger than 100  $\mu\text{m}$  shown in Fig. 7e) with  $G(t)$  for HB-2 yield properties of a composite. No particle contact is allowed, corresponding to the assumption that all particles are coated by the polymer (with a minimum of 6 binder MP between particles). Validity of this assumption will be indirectly confirmed by excellent agreement of simulated results with experimental data.

**Table 2.** Material parameters of the PBX-9501

Binder		
	Bulk Modulus $K$	3.6 GPa
	Shear Modulus $G$	$\sum G_i e^{-t/\tau_i}$ see ref [17] for coefficients
	Density $\rho$	1.48 g/cm <sup>3</sup>
HMX Particle		
	Bulk Modulus $K$	13.4 GPa
	Shear Modulus $G$	5.84 GPa
	Density $\rho$	1.85 g/cm <sup>3</sup>

From the investigation of the sensitivity of composite properties on material point resolution shown in Fig. 2 and Fig. 3 we obtained that  $\Delta G(t)/G(t) \sim S/(AR)$ . For HB-1,  $(G^{\text{filler}}/G^{\text{binder}}) \approx 10^4$  at  $t=10$  ms. To achieve  $\Delta G(t)/G(t)$  about 20% accuracy at  $(G^{\text{filler}}/G^{\text{binder}}) \approx 10^4$ , we need resolution  $R=16$

MP/mm for the model system shown in Fig. 2. The ratio of S/A of HB-1 to that of the model composite shown in Fig. 2 is about 678. Thus we need  $16 \times 678 = 10848$  MP/mm resolution for the HB-1 to achieve the 20% accuracy provided that fillers are separated by at least 4 MP. In order to validate applicability of this relation derived for model composite to the PBX composite, HB-1 was simulated at various resolutions from 2083 MP/mm to 25000 MP/mm as shown in Fig. 8. As expected increase in MP resolution leads to softer composite modulus. In agreement with our estimates from model composites, increase in material point resolution from 12500 MP/mm to 25000 MP/mm does not change composite properties. It is noticeable that at resolution of 2083 MP/mm, the simulated shear modulus is exceptionally high. This is because that the resolution is so low that the particles in HB-1 are bridged with an artificially stiffer interfacial binder.

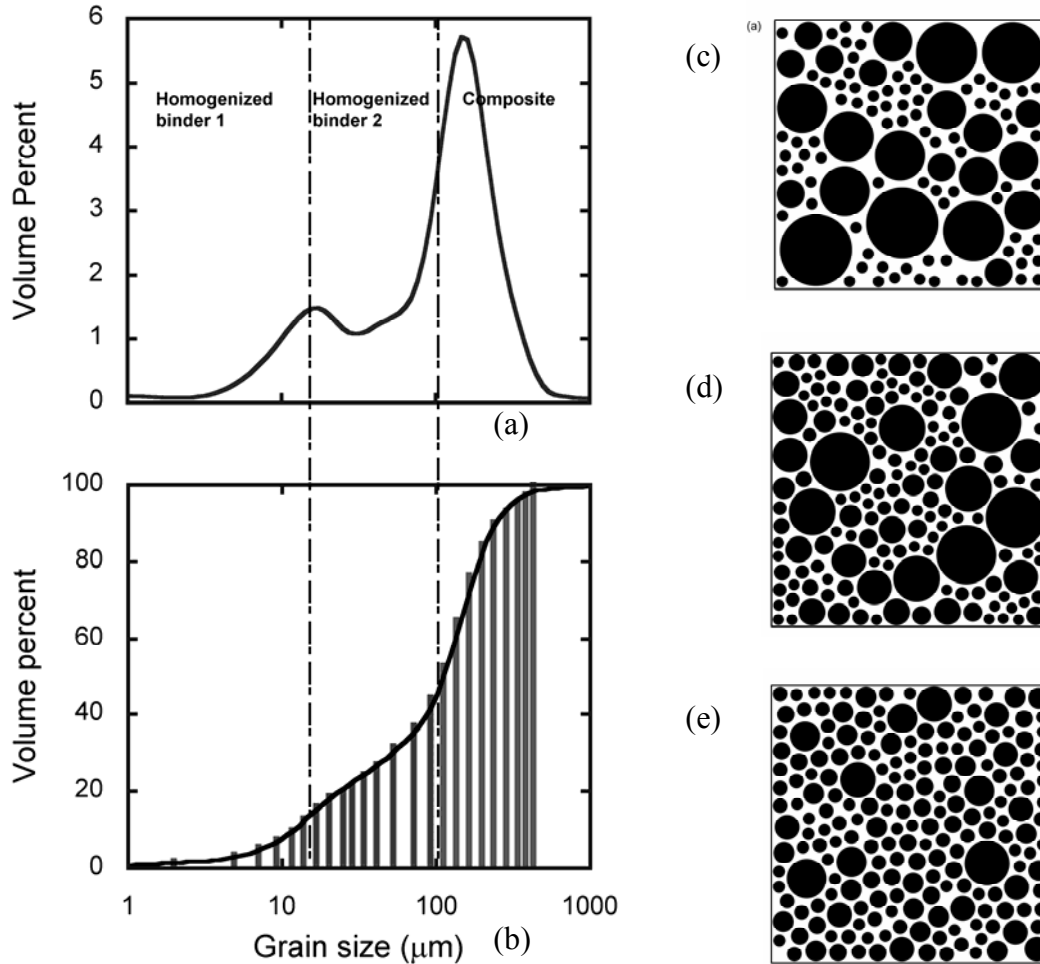


**Figure 7.** Illustration of the division of the HMX grains into three class sizes and corresponding packed structures. (a) Particle size distributions of HMX. (b) Integrated particle size distributions of HMX. Line – experimental data, bars – simulation data. (c) Homogenized binder 1. Length of the box: 0.048 mm. Particle volume fraction: 65%. (d) Homogenized binder 2. Length of the box: 0.42 mm. Particle volume fraction: 63%. (e) Composite. Length of the box: 2.75 mm. Particle volume fraction: 52%.

In our PBX-9501 simulations, we divide the time range of interest into 7-8 domains based on the availability of the computational power and the time efficiency, and use different material point masses (from  $10^{-2}$  to  $10^{+5}$  times that corresponding to actual material density for HB-1, for example) for each domain to obtain the corresponding time range of the  $G(t)$  curve. As an example,  $G(t)$  curves

for HB-1 for each mass are shown in Fig. 9. We observe that  $G(t)$  for a given MP mass nicely overlaps that obtained for smaller and larger MP masses, demonstrating the validity of probing various time scale of  $G(t)$  decay by varying material speed of sound via mass variation. Similar results can be seen for HB-2 and PBX-9501 (not shown).

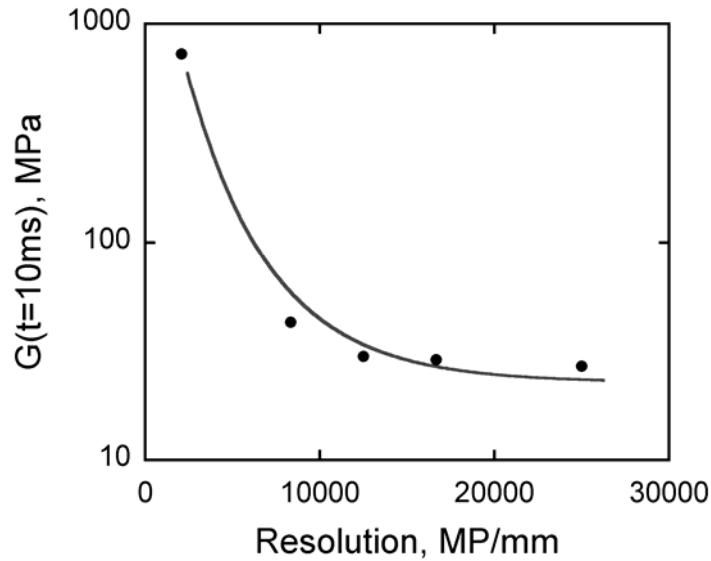


**Figure 8.** Calculated shear modulus at time of 10 ms for homogenized binder 1 as a function of resolution.

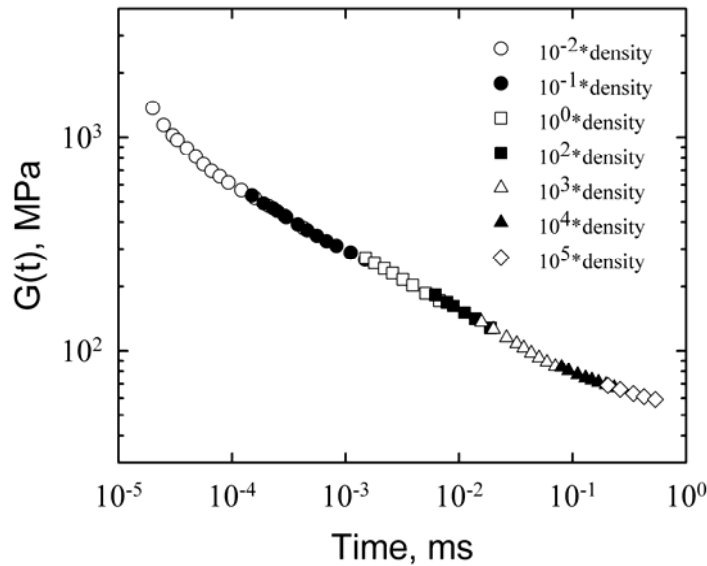


**Figure 9.** Viscoelastic properties of homogenized binder 1 calculated using various material densities to probe various time scales.

Using the three-stage (HB-1, HB-2, PBX-9501) homogenized binder approximation methodology, the upper and lower bounds of time dependent shear modulus of PBX-9501 were computed using stress relaxation and creep simulations, and compared with the experimental data [17] in Fig. 10. We anticipate that  $G(t)$  obtained from our 2-D simulations is similar to the  $G(t)$  which we would obtain from 3-D simulations based on the previous FEM micromechanics simulations for the glass-estane mock PBXs that reported in Ref. [4], which showed no significant difference between

elastic properties predicted by 2-D and 3-D models. Fig. 10 indicates that our MPM composite simulations yield  $G(t)$  in good agreement with experimental data, with MPM yielding a slightly higher modulus at longer times. The predicted lower bound for  $G(t)$  is only 15% higher than the experimental data, which is a much better agreement than seen in previous numerical studies of PBXs [1,2,4-6,18,19].

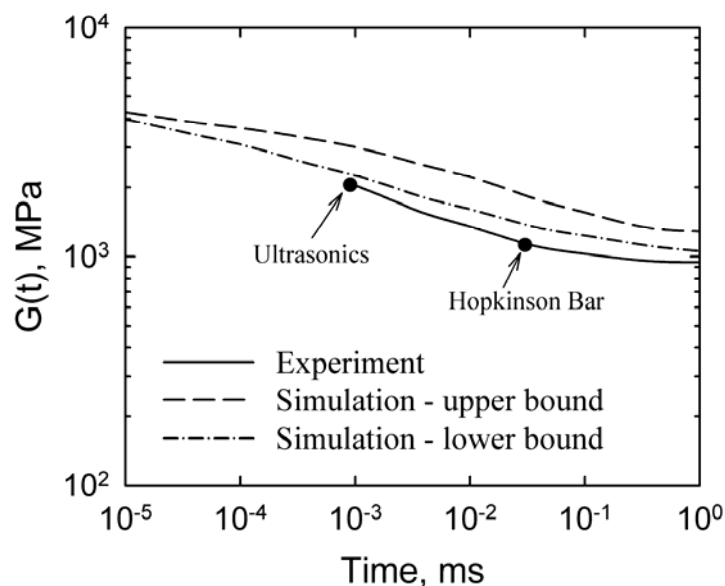


**Figure 10.** Time dependent shear modulus of PBX-9501 from experiments and simulations.

One possible reason for the discrepancy between the predicted  $G(t)$  and experiment is inaccuracy in the experimental data. The explosive nature of PBX-9501 makes the measurement of viscoelastic properties difficult, especially at high frequencies. Another possible source of discrepancy is our simplified representation of the material structure. Simulations are based on theoretically perfect material, that is, the material is randomly packed with no defects, such as cracks, and the HMX particles are perfectly bonded with the polymer matrix. But real materials are certainly not perfect and, therefore, it is possible that the experimental data is lower than the predicted values. Simulations on elastic properties of glass-estane mock PBXs [4] also show that perfect bonding between the particles and the polymer matrix yields higher than experiment results, especially at high volume fractions.

## Conclusion

Viscoelastic properties of polymer bonded explosive material PBX-9501 were studied by Material Point Method (MPM). We proposed and validated a homogenized “dirty” binder approximation to solve the problem of resolving very broad filler size distribution of HMX grains in the PBX-9501 composite. The sensitivity studies of composite properties to the material point resolution showed that insufficient resolution of composites leads to artificially stiff homogenized properties. The error of determining composite modulus from MPM computational experiments was proportional to the interfacial length and inversely proportional to the density of material points (resolution). Reasonable agreement between predicted and experimentally measured  $G(t)$  for PBX-9501 was obtained over 6 orders of magnitude in time.

## Acknowledgement

This work is funded by the University of Utah Center for the Simulation of Accidental Fires and Explosions (C-SAFE), funded by the Department of Energy, Lawrence Livermore National Laboratory, under subcontract B341493. The authors thank fruitful discussion with Scott Bardenhagen, Dmitry Bedrov and Yajun Guo.

## References

1. Banerjee B and Adams O 2003 *Physica B* **338** 8
2. Segurado J and Llorca J 2002 *Mech. And Phys. Solids* **50** 2107
3. Skidmore C B, Phillips D S, Son S F and Asay B W 1998 *Shock Compression of Condensed Matter 1997* (New York: American Institute of Physics) 579
4. Banerjee B, Cady C M and Adams O 2003 *Modelling Simul. Mater. Sci. Eng.* **11** 457
5. Lusti H R, Karmilov I A, Gusev A A 2003 *Soft Materials* **1** 115
6. Lutsi H R, Gusev A. A. 2004 *Modelling Simul. Mater. Sci. Eng* **12** S107
7. Sulsky D, Chen Z and Schreyer H L 1994 *Comput. Methods Appl. Mech. Engrg.*, **118** 179-186.
8. Sulsky D, Zhou S J and Schreyer H L 1995 *Comput. Phys. Commun.*, **87** 236-252.
9. Sulsky D and Schreyer H K 1996 *Comput. Methods. Appl. Mech. Engrg* **139** 409-429.
10. Zhou S 1998 “*The Numerical Prediction of Material Failure Based on the Material Point Method*” Ph.D. Thesis, University of Mexico.
11. Gusev A A 1997 *J. Mech Phys Solids* **45** 1449
12. NairnMPM simulation package is freely available at <http://nairn.mse.utah.edu>. Each element contained 4 material points. Update strain average option was used.
13. Lubachevsky B D and Stillinger F H 1991 *J. Statistical Physics* **64** 561
14. Aklonis J J and MacKnight W J 1983 *Introduction to Polymer Viscoelasticity 2nd Ed.* (New York: Wiley)
15. Jones R M 1999 *Mechanics of Composite Materials 2nd ed.* (Philadelphia: Taylor & Francis)
16. Hughes T J R 2000 *The Finite Element Method* (Mineola: Dover )
17. Bennett J G, Haberman K S, Johnson J, Asay B W and Henson B F 1998 *J. Mech. Phys. Solids* **46** 2303
18. Clements B E and Mas E M 2004 *Modelling Simul. Mater. Sci. Eng.* **12** 407
19. Banerjee B and Adams O 2004 *International Journal of Solids and Structures* **41** 481